

# Intensity distribution of scalar waves propagating in random media

P. Markoš<sup>1,2</sup> and C. M. Soukoulis<sup>1,3</sup>

<sup>1</sup>*Ames Laboratory and Department of Physics and Astronomy, Iowa State University, Ames, Iowa 50011*

<sup>2</sup>*Institute of Physics, Slovak Academy of Sciences, 845 11 Bratislava, Slovakia*

<sup>3</sup>*Research Center of Crete, FORTH, 71110 Heraklion, Crete, Greece*

Transmission of a scalar field through a random medium, represented by a system of randomly distributed dielectric cylinders, is calculated numerically. The system is mapped to the problem of electronic transport in disordered two-dimensional systems. Universality of the statistical distribution of transmission parameters is analyzed in the metallic and localized regimes. In the metallic regime, the universality of transmission statistics in all transparent channels is observed. In the band gaps, we distinguish a disorder induced (Anderson) localization from tunneling through the system, due to a gap in the density of states. We also show that absorption causes a rapid decrease of the mean conductance, but, contrary to the case of the localized regime, the conductance is self-averaged with a Gaussian distribution.

PACS numbers: 41.20.Jb, 72.10.-d, 73.23.-b

## I. INTRODUCTION

Transport of classical waves in random media is a challenging problem, attracting increasing interest of theoretical and experimental physicists because it offers the possibility of studying Anderson localization.<sup>1</sup> Since interactions do not play any role in classical wave scattering, these systems might be more convenient for experimentally verifying the scaling theory of localization<sup>2</sup> than quantum electronic systems, where the influence of the mutual interaction of electrons upon transport has not been yet clarified.<sup>3</sup> Two main issues of localization theory, namely the presence or absence of the metallic state in the two-dimensional (2D) systems, and the validity of the single parameter scaling (SPS)<sup>2,4,5</sup> might be more readily resolved experimentally for the classical wave problem than for the electronic one. Recent experimental results for the transmission of electromagnetic waves indeed confirmed that transmission is universal in the diffusive regime,<sup>6</sup> and presented strong indications for disordered induced Anderson localization.<sup>7,8,9</sup>

In this paper, we analyze numerically the transmission of scalar classical waves through a two dimensional (2D) system of randomly distributed dielectric cylinders. Following Ref. 10, we map the problem into the 2D Anderson model with random binary potential. Statistical properties of wave transmission are then analyzed using the transfer matrix method.<sup>11</sup> We calculate the conductance  $g$  as<sup>12,13</sup>

$$g = \sum_{ab} T_{ab}. \quad (1)$$

In Eq. (1),  $T_{ab} = |t_{ab}|^2$ , where  $t_{ab}$  is the transmission amplitude from channel  $a$  to channel  $b$ .  $a, b = 1, 2 \dots N_{\text{op}}$ , where  $N_{\text{op}}$  is the number of open channels. We first determine the band structure of the original classical wave problem. Then, we analyze the statistical properties of the transmission in bands and gaps.

In bands, where  $g > 1$ , we observed diffusive transport. Statistical properties of the transmission are in

good agreement with theoretical predictions of the random matrix theory<sup>14,15</sup> and the DMPK equation.<sup>16,17</sup> The distribution of the conductance is Gaussian with a universal dimension-dependent variance.<sup>14,18,19,20,21</sup> Universal properties were predicted not only for the conductance  $g$ , but also for the normalized parameters  $s_{ab} = T_{ab}/\langle T_{ab} \rangle$ <sup>22,23</sup> and for the normalized transmission in a given transport channel

$$s_a = \frac{T_a}{\langle T_a \rangle}, \quad T_a = \sum_b T_{ab}. \quad (2)$$

The universal probability distribution

$$p(s_a) = \int_{-i\infty}^{+i\infty} \frac{dx}{2\pi} \exp[xs_a - \Phi(x)] \quad (3)$$

$$\Phi(x) = \langle g \rangle \ln^2 \left( \sqrt{1 + x/\langle g \rangle} + \sqrt{x/\langle g \rangle} \right)$$

has been derived analytically.<sup>24,25</sup> From Eq. (3), the second cumulant is obtained as

$$\text{vars}_a = \langle s_a^2 \rangle - \langle s_a \rangle^2 = \frac{2}{3\langle g \rangle}. \quad (4)$$

Universality of the statistical properties of parameters,  $s_a$ , was confirmed experimentally<sup>6</sup> up to rather small values of the conductance ( $\langle g \rangle \approx 2 - 3$ ).

In gaps, the mean of the logarithm  $\langle \ln g \rangle$  decreases linearly with the system size. Here, we distinguish between two different regimes, one with non-zero density of states, and the other called tunneling regime, characteristic for the frequency region without eigenstates. The first describes Anderson localization, characterized by the Gaussian distribution of  $\langle \ln g \rangle$  with variance  $\text{var} \langle \ln g \rangle \propto -L/\xi$  ( $\xi$  is the localization length) in agreement with localization theory. The second regime appears in the gaps, where the density of states is very small. Then, the transmission is determined by tunneling through the sample. Although  $\langle \ln g \rangle \propto -L$ , the distribution of  $\langle \ln g \rangle$  is not

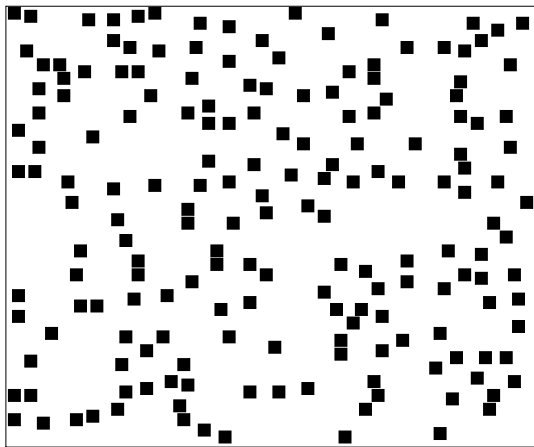


FIG. 1: Typical sample configuration. The size of the system is  $128 \times 128$ , the filling factor  $x = 0.1$ . 182 rectangular rods with square cross-section of  $3 \times 3$  are randomly distributed throughout the sample. Scalar wave propagates from left to the right.

Gaussian but given by the statistics of the energy spectra.

The form of the probability distribution  $p(\ln g)$  enables us also to distinguish between localization and absorption. We find that absorption also gives a decrease of  $\langle \ln g \rangle \propto -L$ ; however, in contrast to localization, the conductance remains self-averaged. Our data agree with the theoretical prediction,<sup>26</sup> as well as with the qualitative criterion<sup>9</sup> for localization  $2/(3\text{vars}_a) \leq 1$ .

The paper is organized as follows: In Sect. II, we introduce the model and system parameters. In Sect. III, we present the mapping of the classical wave problem into the problem of the transmission of electrons in disordered systems.<sup>10</sup> Results of numerical simulations are presented in Sect. IV and V. Conclusions are given in Sect. VI.

## II. MODEL

We study a two-dimensional system consisting of a random array of dielectric cylinders. To make the numerical simulations easier, we consider rectangular rods instead of cylinders. A typical sample is shown in Fig. 1. No contact or overlap of neighboring rods is allowed. The dielectric permittivity of rods is  $\epsilon_2$  and of the embedding medium is  $\epsilon_1$ . Two semi-infinite leads with permittivity  $\epsilon_{\text{lead}}$  are attached to the sample. The concentration of the dielectric rods is given by the filling factor  $x$  of the rod's material. In this work we consider square cross-section of dielectric  $3 \times 3$  rods, measured in dimensionless units. In the same units, the system size  $L$  varies from 32 up to 256.

## III. MAPPING TO THE ELECTRONIC SYSTEM

We use the formal equivalence<sup>10</sup> of the scalar wave equation,

$$\nabla^2 u + \epsilon(\vec{r})\omega^2 u = 0, \quad (5)$$

and the Schrödinger equation for electrons,

$$\nabla^2 \Psi + [E - V(\vec{r})] \Psi = 0, \quad (6)$$

(we set  $2mc^2/\hbar^2 = 1$  and  $c^2 = 1$ ). For a given space dependence,  $\epsilon(\vec{r})$ , and given frequency,  $\omega$ , one can find a potential  $V(\vec{r})$  and energy  $E$  such that the solutions  $u$  and  $\Psi$  of Eqs. (5) and (6) are identical. Formal equivalence requires that the identity

$$\omega^2 \epsilon(\vec{r}) = E - V(\vec{r}) \quad (7)$$

must be fulfilled for all  $\vec{r}$ .

Formula (7) does not mean that the two models described by Eqs. (5) and (6) are equivalent, because potential  $V(\vec{r})$  depends both on the frequency,  $\omega$ , and the energy,  $E$ . Equation (7) only means that for a given scalar wave model defined by  $\epsilon(\vec{r})$ , we can find for each frequency,  $\omega$ , an electronic model with potential  $V(\vec{r})$  and energy  $E$ , that the solutions of both models are the same.

Both the energy and the potential of the electronic model are fixed by formula (7). Changing the frequency,  $\omega$ , we obtain another electronic model, since the potential  $V(\vec{r})$  changes. This means that for a given spatial distribution of  $\epsilon(\vec{r})$ , two different frequencies,  $\omega$ , define two different electronic models.

To be more specific, we consider a model of randomly distributed rectangular rods discussed in Sect. II. This model can be mapped into the electronic model with a random binary potential. For a given sample, the spatial distribution of the potential is identical with the distribution of the permittivity. The energy,  $E$ , as well as two values of the potential,  $V_1$  and  $V_2$ , is determined by Eq. (7) with the following relations

$$\omega^2 \epsilon_{\text{lead}} = E \quad (8)$$

$$\omega^2 \epsilon_1 = E - V_1 \quad (9)$$

$$\omega^2 \epsilon_2 = E - V_2. \quad (10)$$

From Eqs. (9) and (10) we easily obtain

$$\omega^2 \epsilon_1 = \frac{\delta}{\mu - 1}, \quad (11)$$

where

$$\mu = \frac{\epsilon_2}{\epsilon_1} \quad (12)$$

and

$$\delta = V_2 - V_1, \quad (13)$$

The energy,  $E$ , is given as

$$E = V_1 + \frac{\delta}{\mu - 1}, \quad (14)$$

and  $V_1$  is determined by

$$V_1 = \omega^2(\epsilon_1 - \epsilon_{\text{lead}}). \quad (15)$$

Note that for  $\epsilon_{\text{lead}} = \epsilon_0 = 1$  (vacuum in leads), Eqs. (8), (9, and (10) can be solved only when both  $V_1, V_2 > 0$  assuming that  $\epsilon_1, \epsilon_2 > 1$ .

For simplicity, we consider in this paper the special case,

$$\epsilon_1 = \epsilon_{\text{lead}} = 1. \quad (16)$$

The method is, of course, applicable to any set  $(\epsilon_{\text{lead}}, \epsilon_1, \epsilon_2)$ , including  $\epsilon_{\text{lead}} > \epsilon_1$ .

Using Eqs. (15) and (16), we have  $V_1 \equiv 0$ . Comparison of Eq. (11) and Eq. (14) gives  $\omega^2 = E$ . Finally,  $V_2 = -\delta$ . We also fix the ratio of two permittivities  $\mu = \epsilon_2/\epsilon_1$ , to the value of  $\mu = 11$ .

In numerical simulations, we used the discretized version of the Schrödinger equation, Eq. (6),

$$\Psi_{x,y+1} + \Psi_{x,y-1} + \Psi_{x+1,y} + \Psi_{x-1,y} = (4 - E + V_{xy})\Psi_{xy}. \quad (17)$$

Hard wall boundary conditions were used. The transfer matrix method<sup>11</sup> was used to calculate numerically all the parameters,  $s_a$ , and the conductance. The number of open channels,  $N_{\text{op}} \leq L$ , which enters in Eq. (1) is given by the number of propagating solutions ( $k_n$  real) of the dispersion relation

$$2 \cos k_n = 4 - E - 2 \cos \frac{\pi}{L+1} n, \quad n = 1, 2, \dots, L. \quad (18)$$

Each frequency,  $\omega$ , defines a corresponding tight-binding Hamiltonian, for which the transmission is calculated using standard numerical procedures known for the electronic localization problems.<sup>11</sup> Statistical ensembles of  $N_{\text{stat}} = 10^4$  samples were considered, which assure that sufficient accuracy of the transmission parameters of interest were obtained.

#### IV. CONDUCTANCE

Figures 2 and 3 show the  $\omega$  dependence of the mean conductance for the present model. Equivalently, the numerical results of Figs. 2 and 3 might be interpreted as the  $\delta$ -dependence of the conductance of the 2D electronic system. In the last case, however, one must keep in mind that in the Anderson model, the value of  $\delta$  determines the random potential. Data presented in Figs. 2 and 3 do not directly correspond to the electronic density of states in the disordered electronic system. Different values of  $\delta$  correspond to different models. Note also that the energy,  $E$ , Eq. (14) is also a function of  $\delta$ .

For completeness, we show in Fig. 4 the density of states,  $\rho(E)$ , of the electronic system for four values of  $\delta$ .

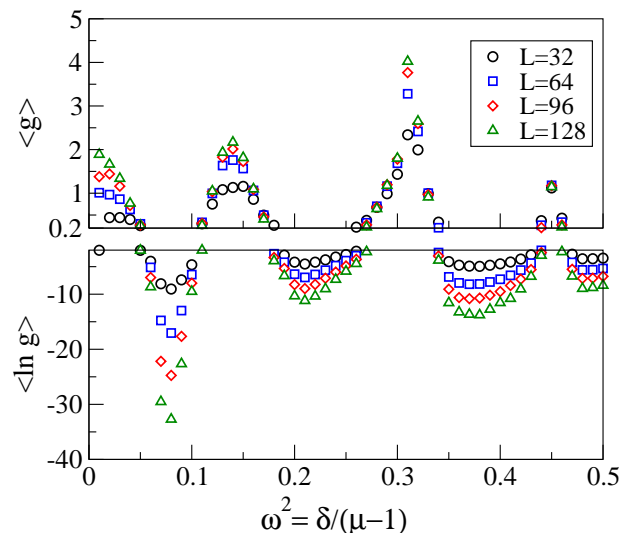


FIG. 2: Mean conductance  $\langle g \rangle$  (top) and  $\langle \ln g \rangle$  (bottom) as a function of the frequency for  $\mu = \epsilon_2/\epsilon_1 = 11$  and  $x = 0.2$ . Frequency bands and gaps are clearly visible. In bands around  $\omega^2 = 0.14$  and  $0.31$ , we find transport statistics typical for the metallic regime. Two different transport regimes were observed in gaps: In the first gap,  $\omega^2 \approx 0.08$ , the density of states is very small and transport is due to tunneling through the sample. In the second gap,  $\omega^2 \approx 0.21$ , we observed disorder induced Anderson localization.

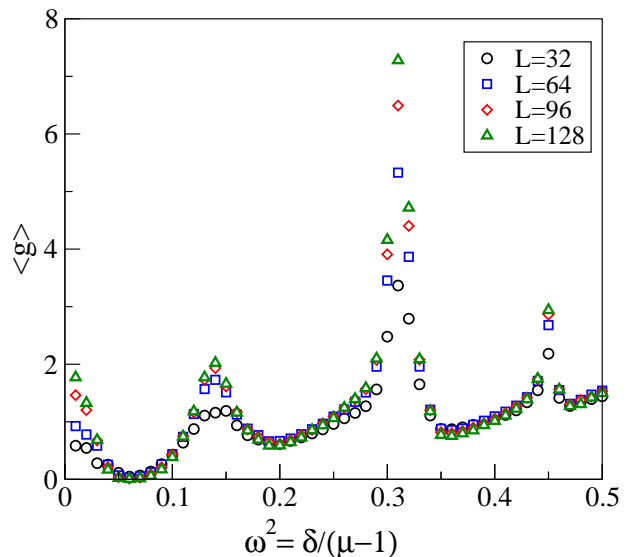


FIG. 3: The same as in Fig. 2, but for  $x = 0.1$ .

##### A. Diffusive regime ( $\langle g \rangle > 1$ )

Three frequency bands are visible in Figs. 2 and 3, where we expect the metallic behavior. Mean conductance  $\langle g \rangle > 1$  slightly increases with the system size and the value of  $\text{var } g$  is very close to the universal conductance fluctuation.<sup>18,20,21</sup> The distribution of the conductance is Gaussian (see, for example, Fig. 11). Although

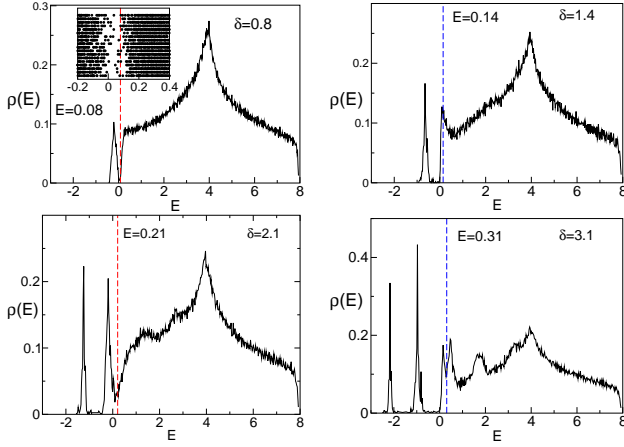


FIG. 4: Density of states of the electronic system with  $x = 0.2$  calculated for four values of  $\delta$ . The size of the system is  $48 \times 48$  and an average over 10 ensembles was calculated. Dashed lines indicate the energy,  $E(\delta)$ . For  $\delta = 0.8$ , the inset shows the position of eigenenergies for 18 different samples.

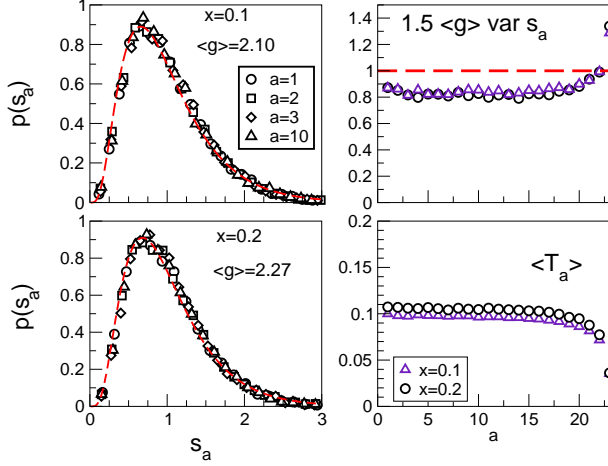


FIG. 5: Left panels: Probability distribution  $p(s_a)$  for some open channels compared with the theoretical prediction of Eq. (3) (dashed line).  $\omega^2 = 0.14$  (the center of the first band). Concentration of cylinders is  $x = 0.1$  (top) and  $x = 0.2$  (bottom). Right panels: The second cumulant  $\frac{3}{2}\langle g \rangle \text{var } s_a$  as a function of index  $a$  (top) and mean values  $\langle T_a \rangle$  (bottom). The size of the system is  $L = 192$ , electron energy is  $E = 0.14$ , the number of open channels,  $N_{\text{op}} = 23$ . Statistical ensemble of  $N_{\text{stat}} = 10000$  samples was considered.

these properties are finite size effects (no metallic state exists in 2D in the limit  $L \rightarrow \infty$ ), the numerical data enable us to check the theoretical prediction about the transmission statistics.

In Fig. 5 we show the statistics of the parameters,  $s_a$ , for the frequency in the center of the first ( $\delta \approx 1.4$ ) band. The number of open channels is 23 for the size of the system  $192 \times 192$ . Results confirm that the distribution,  $P(s_a)$ , is universal and does not depend on  $a$ . The second cumulant,  $\text{var } s_a$ , is close to its theoretical value,

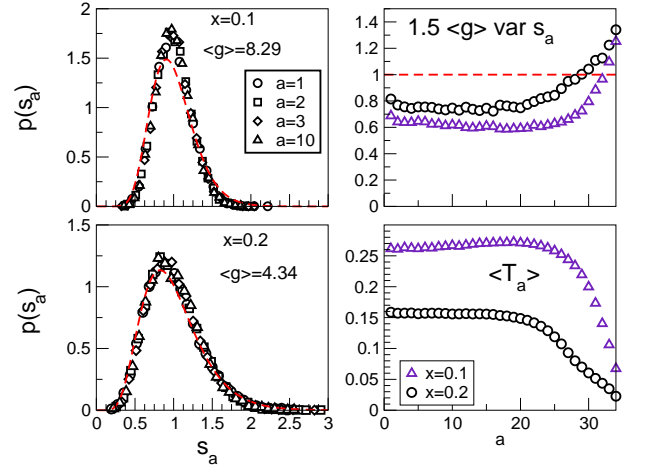


FIG. 6: The same as in Fig. 5, but for  $\omega^2 = 0.31$ .  $N_{\text{op}} = 34$ . The agreement with theory is not as good as in Fig. 5, especially for  $x = 0.1$  because of the small system size.

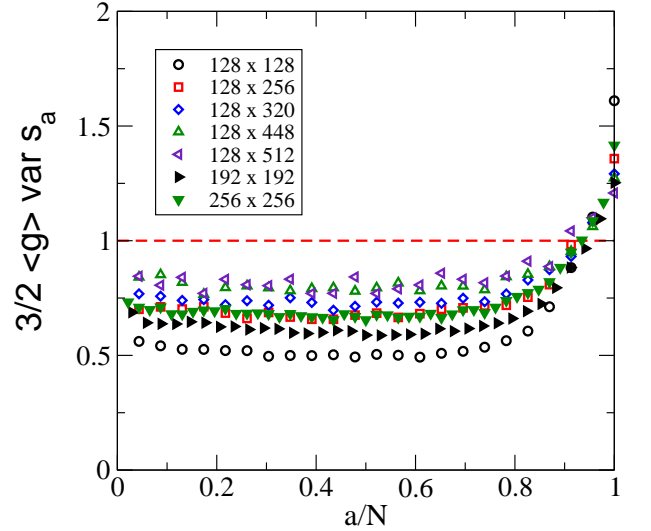


FIG. 7: The second cumulant  $\frac{3}{2}\langle g \rangle \text{var } s_a$  as a function of index  $a$  for the center of the second band  $\omega^2 = 0.31$  and  $x = 0.1$ . 2D systems of size  $L \times L$  with  $L = 125, 192$  and  $256$  were considered. These results are compared with quasi-one dimensional systems of size  $128 \times L_z$  with  $L_z = 128, 256, 320, 448$  and  $512$  with mean conductance  $\langle g \rangle = 7.28, 4.29, 3.53, 2.57$  and  $2.25$ , respectively.

$2/3\langle g \rangle$ .

The same analysis was completed for the second band (Fig. 6). Here, the agreement with theory is not as good as in the previous case, presented in Fig. 5 especially for a smaller concentration of rods. Although the distribution,  $P(s_a)$ , does not depend on  $a$ , it differs considerably from theoretical predictions. We interpret this discrepancy as a finite size effect. Indeed, the mean conductance  $\langle g \rangle$  increases with the system size (Fig. 3, and inset of Fig. 8), which indicates that we have not reached the diffusive regime yet.

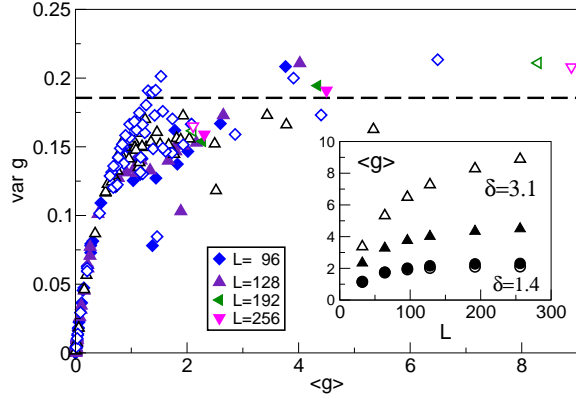


FIG. 8: The variance of the conductance,  $\text{var } g = \langle g^2 \rangle - \langle g \rangle^2$ , as a function of the mean conductance for  $x = 0.1$  and  $x = 0.2$ , and various system sizes. Open symbols:  $x = 0.1$ , full symbols:  $x = 0.2$ . For small values of  $\langle g \rangle$ , the numerical results scale to a universal curve. For large  $\langle g \rangle$  they converge to the universal value of  $\text{var } g = 0.1855$ .<sup>18,20</sup> The inset shows the mean conductance  $\langle g \rangle$  for  $\delta = 1.4$  (circles) and  $\delta = 3.1$  (triangles). For  $\delta = 3.1$ ,  $\langle g \rangle$  still increases with  $L$ , which indicates that  $L$  is not large enough for transport to be diffusive.

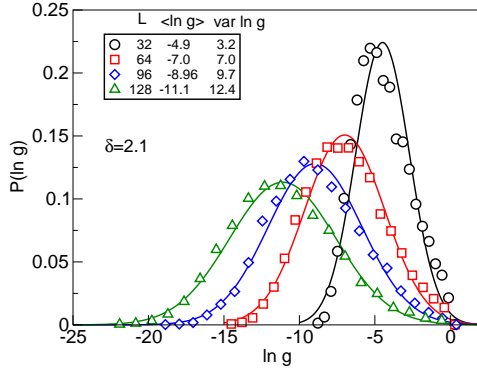


FIG. 9: The probability distribution  $P(\ln g)$  for  $\omega^2 = 0.21$ . The distribution is close to the log normal with  $\text{var } \ln g \approx -\langle \ln g \rangle$ , typical behavior of Anderson localization. The number of random configurations  $N_{\text{stat}}$  is  $10^5$  for  $L \leq 96$  and  $10^4$  for  $L = 128$ . The legend presents the data for  $\langle \ln g \rangle$  and  $\text{var } \ln g$ .

Note also that we are studying 2D samples, while the theory is formulated for quasi one dimensional systems. Therefore, we expect that the agreement with theory should be better if the length of the system increases. This is confirmed by numerical results presented in Fig. 7, which shows the second cumulant  $\frac{3}{2}\langle g \rangle \text{var } s_a$  for various 2D and quasi one dimensional system.

Figure 8 shows the variance,  $\text{var } g$ , of the conductance vs the mean conductance  $\langle g \rangle$ . We expect that  $\text{var } g$  should saturate to the universal value of  $\text{var } g \rightarrow 0.1855$  [18,20] for  $g \gg 1$ .

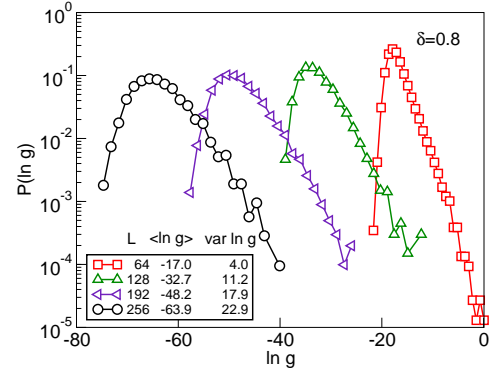


FIG. 10: The probability distribution  $p(\ln g)$  for  $\omega^2 = 0.08$  and  $x = 0.2$ . The distribution shows that transport is due to tunneling through a system with an energy gap. Note that the width of the distribution,  $\text{var } \ln g \ll \langle \ln g \rangle$ , is much smaller than that of the disorder induced insulator. Data for the mean value and variance of  $\ln g$  are given in the legend.  $N_{\text{stat}} = 7000$  for  $L \leq 256$  and is  $> 10^4$  for smaller  $L$ .

### B. Localization ( $\langle g \rangle \ll 1$ )

In the regions between the pass bands, the conductance decreases exponentially with the system size. It is much more pronounced for larger concentrations of cylinders ( $x = 0.2$ ). Here, two different regimes were observed.

In the upper gap, ( $\delta \approx 0.21$ ) the observed statistical properties of the conductance are in agreement with the theoretical expectations for the localized regime: The distribution of  $\ln g$  is Gaussian (Fig. 9) with  $\text{var } \ln g \approx -\langle \ln g \rangle \propto 2L/\xi$ , which is characteristic for the disorder induced localization. The parameter  $\xi$  is the localization length.<sup>27</sup>

In the lower gap ( $\delta \approx 0.08$ ), the conductance decreases rapidly as the size of the system increases. The probability distribution of  $\ln g$  is not Gaussian, as can be seen in Fig. 10. Instead, it decreases exponentially for larger values of conductance as

$$p(\ln g) \propto \exp \text{const}[\langle \ln g \rangle - \ln g]. \quad (19)$$

In contrast to Anderson localization, no samples with conductance close to 1 were found. This indicates that transport is possible only by tunneling through isolated eigenstates. Also, the variance,  $\text{var } \ln g$ , is much smaller than that of the Anderson insulator,

$$\text{var } \ln g \ll -\langle \ln g \rangle. \quad (20)$$

The last property seems to be in agreement with previous work of Deych *et al.*<sup>28</sup> who argued that single parameter scaling does not work in the energy intervals, where the density of states is so small that another characteristic length  $l_s \sim \sin^{-1} \rho(E)$  exceeds the localization length. Indeed, we found that the density of states is close to zero in the neighborhood of  $E = 0.08$  (Fig. 4), so that the average distance between isolated eigenstates is larger than the localization length ( $\xi \approx 8$  was estimated from

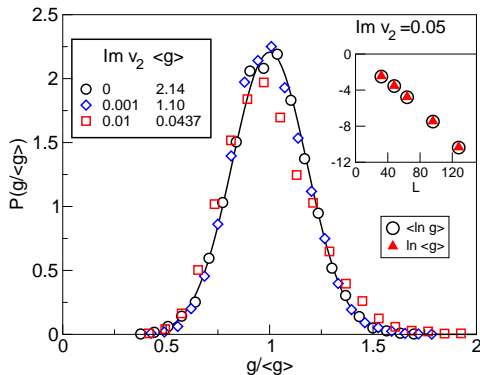


FIG. 11: The probability distribution of the conductance  $g$  for  $x = 0.2$  and  $\omega^2 = 0.14$  for the case without absorption and with small absorption in the dielectric cylinders ( $L = 128$ ). Absorption is due to the small imaginary part of the permittivity  $\epsilon_2$  of cylinders. The mean conductance decreases, due to absorption (see legend) and the conductance distribution is Gaussian. The inset shows the  $L$  dependence of  $\ln \langle g \rangle$  and  $\langle \ln g \rangle$  for the stronger absorption ( $\text{Im } V_2 = 0.05$ ). The numerical results confirm that the conductance is self-averaged.

the  $L$  - dependence  $\langle \ln g \rangle$ . For instance, in the interval  $0.05 < E < 0.11$ , we found an average of only one eigenstate, when  $L = 48$  so that  $l_s > 48$ . Although  $l_s$  is expected to decrease when  $L$  increases, we were not able to reach Anderson localization, even for the largest system studied,  $L = 256$ .

## V. ABSORPTION

Absorption reduces the transmission of the EM waves in a similar way as localization. Mean conductance decreases exponentially with the system length.<sup>26</sup> To distinguish between Anderson localization and absorption effects, we need to understand the statistical properties of the transmission. In Ref. 9 the simple criterion for localization was derived, based on the value of the parameter

$$g' = 2/(3\text{vars}_a). \quad (21)$$

It was argued that localization appears if  $g' \leq 1$ .

To study the effects of absorption, we add a small imaginary part to the permittivity of cylinders (more precisely,  $V_2$  in Eq. (10) becomes complex in our simulations). First, we analyze how absorption changes the transmission properties of the metallic system. We use  $\delta = 1.4$  and  $x = 0.2$  (Fig. 2). As expected, the mean conductance decreases when the system size increases,  $\langle \ln g \rangle \sim -L$  similarly as for localized waves. In contrast to the localized regime, the conductance is self-averaged in this case,  $\langle \ln g \rangle = \ln \langle g \rangle$ . The conductance distribution is still Gaussian. As shown in Fig. 11, the width of the distribution of the *normalized* conductance depends only weakly on the absorption strength. This is in agreement with analytical results of Brouwer.<sup>26</sup>

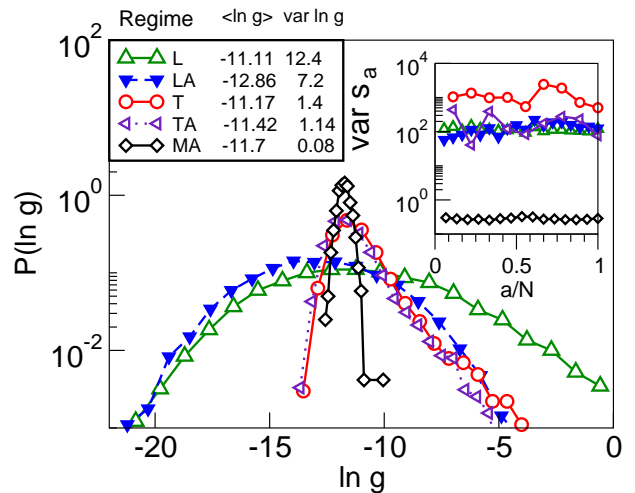


FIG. 12: The probability distribution of the logarithm of the conductance in various regimes. L: regime of Anderson localization with Gaussian distribution and  $\text{var } \ln g \approx -\langle \ln g \rangle$ . LA: localized regime with absorption ( $\text{Im } V_2 = 0.01$ ). Compared with L, we see that the part of the distribution with relatively large conductance is missing. T: tunneling regime, in which  $\text{var } \ln g \ll -\langle \ln g \rangle$ . TA: tunneling with absorption ( $\text{Im } V_2 = 0.05$ ). Absorption does not influence  $p(\ln g)$ . MA: metallic regime with absorption ( $\text{Im } V_2 = 0.065$ ). Here, conductance is self-averaged. Parameters of systems were chosen such that  $\langle \ln g \rangle$  is approximately the same for all systems (see legend). Inset shows  $\text{var } s_a$  in all the above regimes. As predicted in Ref. 9,  $\text{var } s_a < 1$  in the metallic regime with absorption, but is  $\gg 1$  in the localized regime, both with and without absorption. The same holds for the tunneling regime (data for L, LA and TA regimes are almost indistinguishable). Thus, the criterion  $g' < 1$  cannot distinguish between localization and tunneling.

Figure 12 compares the statistics of the logarithm of the conductance of five different transport regimes – localization and tunneling with and without absorption, and diffusive (metallic) regime with absorption. The numerical results confirm that absorption does not change the statistical properties of the conductance, given mostly by the interference of electrons or classical waves due to disorder. In the regime of Anderson localization, the probability to find relatively large values of  $g$  is reduced due to absorption, while another part of the distribution, where  $\ln g \ll \langle \ln g \rangle$ , is almost unaffected by the presence of absorption. As a result,  $p(\ln g)$  is not Gaussian anymore. In the tunneling regime, absorption only reduces the magnitude of  $\text{var } s_a$  as can be seen in the inset of Fig. 12.

## VI. CONCLUSIONS

We presented a numerical analysis of the transmission of the scalar classical wave through a disordered two dimensional system. By mapping this system to a 2D electronic disordered problem, we found frequency inter-

vals with high transmission. For these frequencies, we obtained the statistical distribution of the transmission parameters predicted recently by the theory. We confirmed the universality of the conductance fluctuations and of the distribution of the parameters  $s_a$  in the metallic regime. The universality survives for rather small values of conductance,  $\langle g \rangle = 1 - 3$ . Our numerical results confirm that the theory, developed for the quasi one dimensional systems, can be successfully applied to 2D systems, too. Our results are also consistent with previous experiments.<sup>6</sup>

As there is no metallic regime in two dimensional systems, the above described metallic behavior is just an effect of the finite size of our sample. By increasing the system size, conductance would decrease and finally, in the limit of  $L \gg$  localization length, the wave becomes localized. The localized regime was also observed in a gap, where the density of states is smaller than in the bands, but still non-zero. In this frequency interval, broad distribution of the logarithm of the conductance, typical for the Anderson localization in electronic systems, is observed.

Anderson localization should be distinguish from the

tunneling regime, which we found in the frequency gap, where the density of states is close to zero. Here, the statistics of conductance is determined by the statistical properties of the isolated frequencies inside the gap. The distribution  $p(\ln g)$  differs considerably from Gaussian. These results are in agreement with the theoretical analysis of Deych *et al.*<sup>28</sup>

Finally, we analyzed the effects of absorption. We found, in agreement with theoretical and experimental works, that absorption does not change the statistical properties of the transmission. Since the statistical properties of the parameters,  $s_a$ , are insensitive to the presence of absorption both in the localized and in the metallic regimes, typical values of  $\text{var } s_a$  enable us to decide whether the exponential decrease of the conductance is due to localization or to absorption. However, statistics of  $s_a$  can not distinguish between Anderson localization and tunneling. Fortunately, these two regimes are distinguishable from the form of the probability distribution of the total transmission  $g$ .

**Acknowledgments.** This work was supported by Ames Laboratory (Contract. No. W-7405-Eng-82), and VEGA (Project No. 2/3108/2003).

- 
- \* E-mail: Peter.Markos@savba.sk
- <sup>1</sup> P. W. Anderson, Phys. Rev. **109**, 1492 (1958)
  - <sup>2</sup> E. Abrahams, P. W. Anderson, D. C. Licciardello, T. V. Ramakrishnan, Phys. Rev. Lett. **42**, 673 (1979)
  - <sup>3</sup> E. Abrahams, S. V. Kravchenko, M. P. Sarachik, Rev. Mod. Phys. **73**, 251 (2001)
  - <sup>4</sup> A. MacKinnon and B. Kramer, Z. Phys. B **53**, 1 (1983)
  - <sup>5</sup> K. Slevin, P. Markoš, and T. Ohtsuki, Phys. Rev. Lett. **86**, 3594 (2001); Phys. Rev. B **67**, 155106 (2003)
  - <sup>6</sup> M. Stoytchev and Z. Z. Genack, Phys. Rev. Lett. **79**, 309 (1997)
  - <sup>7</sup> A. Z. Genack and N. Garcia, Phys. Rev. Lett. **66**, 2064 (1991)
  - <sup>8</sup> A. A. Chabanov and A. Z. Genack, Phys. Rev. Lett. **87**, 153901 (2001)
  - <sup>9</sup> A. A. Chabanov, M. Stoytchev and A. Z. Genack, Nature **404**, 850 (2000)
  - <sup>10</sup> C. M. Soukoulis, E. N. Economou, G. S. Grest, and M. H. Cohen, Phys. Rev. Lett. **62**, 575 (1989)
  - <sup>11</sup> T. Ando, Phys. Rev. B **44**, 8017 (1989); J. B. Pendry, A. MacKinnon, P. J. Roberts, Proc. R. Soc. London A **437**, 67 (1992)
  - <sup>12</sup> R. Landauer, IBM Res. Dev. **1**, 223 (1957)
  - <sup>13</sup> E. N. Economou and C. M. Soukoulis, Phys. Rev. Lett. **46**, 618 (1981)
  - <sup>14</sup> C. W. J. Beenakker, Rev. Mod. Phys. **69**, 731 (1997)
  - <sup>15</sup> M. C. W. van Rossum and Th. M. Nieuwenhuizen, Rev. Mod. Phys. **71**, 313 (1999)
  - <sup>16</sup> P. A. Mello, P. Pereyra and N. Kumar, Ann. Phys. (NY) **181**, 290 (1988)
  - <sup>17</sup> P. A. Mello and A. D. Stone, Phys. Rev. B **44**, 3559 (1991)
  - <sup>18</sup> P. A. Lee, A. D. Stone, and H. Fukuyama, Phys. Rev. B **35**, 1039 (1987)
  - <sup>19</sup> Y. Imry, Europhys. Lett. **1**, 249 (1986)
  - <sup>20</sup> M. Rühländer, P. Markoš and C. M. Soukoulis, Phys. Rev. B **64**, 172202 (2001)
  - <sup>21</sup> I. Travěnek, Phys. Rev. B **69**, 033104 (2004)
  - <sup>22</sup> A. Yamilov, H. Cao, Phys. Rev. E **70**, 037603 (2004)
  - <sup>23</sup> E. Kogan, M. Kaveh, R. Baumgartner and R. Berkovits, Phys. Rev. B **48**, 9404 (1993).
  - <sup>24</sup> Th. M. Nieuwenhuizen and M. C. W. van Rossum, Phys. Rev. Lett. **74**, 2674 (1995)
  - <sup>25</sup> E. Kogan and M. Kaveh, Phys. Rev. B **52**, R3813 (1995)
  - <sup>26</sup> P. W. Brouwer, Phys. Rev. B **57**, 10526 (1998)
  - <sup>27</sup> Strictly speaking,  $p(\ln g)$  is not exactly Gaussian in localized regime, see P. Markoš, Phys. Rev B **65**, 104207 (2002) for details.
  - <sup>28</sup> L. I. Deych, M. V. Eremenchouk, A. A. Lisiansky, A. Yamilov, and H. Cao, Phys. rev. B **68**, 174203 (2003) and references therein.